



Time-varying carrier frequency offset estimation in OFDM underwater acoustic communication[☆]



Gilad Avrashi, Alon Amar*, Israel Cohen

Andrew and Erna Viterby Faculty of Electrical and Computer Engineering, Technion – Israel Institute of Technology, Technion City, Haifa 3200003, Israel

ARTICLE INFO

Article history:

Received 8 January 2021

Revised 13 July 2021

Accepted 22 August 2021

Available online 11 September 2021

Keywords:

Multicarrier communication

Carrier frequency offset

Underwater acoustic communication

Time-varying channel

ABSTRACT

We consider the problem of carrier frequency offset estimation in OFDM underwater acoustic communication. In our previous work, we suggested transmitting equi-power and equi-spaced pilot tones which led to a simple carrier frequency offset estimator. Here, we extend this work in two directions: First, equi-power pilots may result in a large peak to average power at the transmitter. Thus, we propose a method to design the phases of the pilot tones so as to keep the peak to average power low, while still obtaining large enough pilot to data ratio needed to decode the pilot symbols. The design method is based on ideas adopted from phase retrieval techniques. Second, we modify the previous carrier frequency offset estimators to the case of a time-varying underwater acoustic channel. These modifications are based on modeling the carrier offset by polynomial and piece-wise models. The estimators use the correlations and intervals between the pulses, and approximate the frequency offsets by small order polynomials. Simulations results show that for constant offsets, the proposed estimators achieve similar performances as state-of-the-art techniques, while for time-varying offsets the proposed estimators are superior.

© 2021 Elsevier B.V. All rights reserved.

1. Introduction

Carrier frequency offset (CFO) in orthogonal frequency division multiplexing (OFDM) communication systems may cause inter-carrier interference, which degrades the performance of OFDM decoders [1,2]. Over the past decades, numerous techniques were proposed to estimate frequency offsets in OFDM, focusing mainly on radio communication channels. These methods can be classified into two categories. The first category of CFO estimators, known as data-aided estimators [4–7], rely on pilot symbols, which are periodically transmitted. The second category, known as blind estimators, does not employ additional training data, but relies solely on the received OFDM data to estimate the CFO using statistical characteristics of the measurements, such as the cyclic prefix segment [8,9], frequency measurements at null subcarrier [10–13], second order statistics, and high order statistics of frequency measurements [14,15].

Unlike the radio communication channel, the time variations of the underwater acoustic communication (UAC) channel are non-

negligible with respect to the propagation speed and are subject to multipath effects, ultimately causing non-uniform Doppler shifts [16,17]. These fast variations of the channel result in short coherence time. On the other hand, the UAC suffers from inherently limited bandwidth which places a lower bound to the block duration. Therefore, limiting the duration of OFDM blocks, in order not to exceed the coherence time [19], has implications on either the system bitrate or its channel robustness [20]. These fast variations have encouraged UAC modem designers to use block-by-block frequency estimators. Accordingly, a coarse Doppler scale compensation is conducted for the entire package, followed by block-by-block estimation of the residual frequency shifts in each block, disregarding neighbor blocks and their estimations.

Li et al. [17] introduced a nonlinear least-squares (LS) CFO estimator using null symbols in the frequency domain by introducing a minimum energy optimization criterion. The authors also employed the LS principle with equi-spaced pilot symbols in each block, which are also used to estimate the channel impulse response (CIR), the concept was later adopted and expanded by Abdelkareem et al. [18]. Both methods require a grid search in the frequency domain and thus suffer from high computational burden on the modem. Carracosa and Stojanovic [22] suggested a block-to-block processing approach for UAC OFDM systems, where the non-uniform phase offset is tracked from one block to the subsequent. Although having the advantage of lower computational complexity, this method requires a fairly slow varying channel over two

[☆] This research was supported by the Pazy Research Foundation and the ISF-NSFC joint research program (Grant no. 2514/17).

* Corresponding author.

E-mail addresses: amar@technion.ac.il (A. Amar), icohen@ee.technion.ac.il (I. Cohen).

consecutive OFDM blocks, which limits the design and results in bitrate loss.

Recently, low complexity CFO estimators for OFDM in UAC channel have been suggested [23–25] that replace the need for exhaustive grid search. Using not only equi-spaced pilot tones in the frequency domain, but also set them to be identical, results in a periodic time-domain block with a period equal to the number of pilot tones. After retaining the channel-independent part of each periodic segment, a small-size correlation matrix between these parts is constructed. The problem of estimating the CFO given this correlation matrix is shown to have a closed form and can be solved efficiently, given that the CFO is constant during the time of one block. These estimators, however, suffer from two drawbacks making them hard to be implemented in practical modems: (1) The use of equi-spaced identical pilots results in high peak-to-average power ratio (PAPR). This problem is thoroughly discussed in Amar et al. [23], but a solution is not offered; (2) Like previous CFO estimators, the assumption of having a constant CFO remains and limits the design of the OFDM block, as investigated in Aval and Stojanovic [20].

In order to overcome the time-varying nature of the underwater acoustic channel, differential OFDM was suggested and combined with a partial fast Fourier transform (FFT) technique [27]. This aims to dissect the OFDM block into several sections, which enables to estimate the channel separately, and thus reducing the problem into piecewise constant channels [20]. Han et al. [21] suggested an eigenvalue decomposition to combine the weights of the partial FFT sub-blocks.

In this paper, we propose a transmitter-receiver design that allows closed-form CFO estimation based on the methods in Amar et al. [23], Avrashi et al. [24]. We present two main contributions: (a) The closed-form CFO estimator presented in Amar et al. [23] has an inherent high PAPR, which makes it inapplicable to practical communication systems. Herein, we present a transmitter design that allows to reduce the PAPR, while preserving the pilot-tone features required for the CFO estimator; (b) We present a CFO estimator for time-varying frequency shifts, thus extending the usable block durations (formerly limited by the coherence time) and allowing higher data rates. Furthermore, the proposed method eliminates the need to use overlap-and-add for zero-padded (ZP) OFDM in order to estimate the CFO.

Instead of identical pilots, a method for designing the pilot tones is proposed, such that the time periodicity feature is preserved, while the effect on PAPR is negligible. By looking at pilot design as a phase retrieval problem with a time-domain envelope chosen to satisfy the low PAPR requirement, we are able to derive a tunable design algorithm for the transmitted signal.

For the receiver side, we develop a closed-form time-varying CFO estimator. The method expands the previously developed closed-form constant CFO estimators, which either use a channel-independent correlation matrix [23], a channel-dependent correlation matrix, or a combination of both [24]. The first estimator is based solely on the channel-dependent correlation matrix. First, the eigenvector associated with the maximal eigenvalue of this matrix is used to estimate the phase accumulations between the pilot-signal periods, and then the CFO is estimated using a linear LS estimator given the phases accumulations. The second estimator is a weighted linear LS estimator, given the phases of the minimal eigenvector of the channel independent correlation matrix and the maximal eigenvector of the channel dependent correlation matrix. Finally, the third estimator solves a generalized eigenvalue decomposition (GEVD) problem by considering jointly the two correlation matrices and then performing a similar second step as the previous estimators. Herein, we show that, under certain conditions, these estimators can be adapted to time-varying channels. Numerical simulations indicate that for time-varying channels, the

bit error rate (BER) performance of the OFDM modem is significantly improved by using the proposed method. Furthermore, we show that by applying the proposed pilot-design algorithm, PAPR values are within fractions of dB of the original random pilots design, without compromising the CFO estimation scheme.

The rest of the paper is organized as follows. In Section 2, we define the signal model and describe the problem of estimating both the channel impulse response and carrier frequency offset in OFDM signals. In Section 3, we present an overview of the closed form eigenvalue decomposition (EVD) based estimation technique, followed by an analysis of both the cost function and the tradeoff between a time locality feature, which is desired for the closed-form CFO estimator, and the resulting high peak-to-average power ratio. In Sections 4 and 5, we introduce a transmitter-receiver design which allows a practical implementation of the closed-form EVD-based estimator. Section 4 offers a closed form pilot design algorithm which compromises between the contradicting requirements by solving a phase retrieval problem. Section 5 focuses on the CFO estimation at the receiver, where the previously suggested solution is expanded for time-varying frequency offsets using a model-based approach. Finally, simulation results are presented in Section 6.

2. Signal model

Consider a ZP-OFDM block with time duration T and K carriers, where the k th carrier frequency is

$$f(k) = f_0 + k\Delta f, k = 0, \dots, K - 1, \quad (1)$$

with f_0 the lower frequency, and $\Delta f = 1/T$ is the carrier spacing. Let the $K \times 1$ vector of symbols be

$$\mathbf{s} = [s(0), s(1), \dots, s(K - 1)]^T, \quad (2)$$

where $s(k) = e^{j\phi(k)}$. The K carriers are composed of $K - Q \gg Q$ data symbols with $\phi(k) \in \mathcal{S}$ and \mathcal{S} is a pre-defined set of phases (such as the quadrature phase-shift keying (QPSK) constellation). The remaining Q symbols are used as pilots, equi-spaced in frequency with spacing $G = K/Q$, i.e., according to (1) the frequency of the q th pilot carrier is $f(qG)$, $q = 0, 1, \dots, Q - 1$. The $P \times 1$ zero-padded discrete time transmitted signal, where $P = K + L$, is

$$\mathbf{u} = \mathbf{T}_{zp}\tilde{\mathbf{s}}, \quad (3)$$

where $\tilde{\mathbf{s}} = \mathbf{F}_K^H \mathbf{s} = [\tilde{s}(0), \tilde{s}(1), \dots, \tilde{s}(K - 1)]^T$ is the signal in the time-domain, \mathbf{F}_K is a $K \times K$ Fourier matrix with the (m, n) th element given by $\frac{1}{\sqrt{K}} e^{-j2\pi/K mn}$, $\mathbf{T}_{zp} = [\mathbf{I}_K, \mathbf{0}_K \mathbf{0}_L^T]^T$ is a $P \times K$ zero-padding matrix, \mathbf{I}_n is the $n \times n$ identity matrix, $\mathbf{0}_n$ is a $n \times 1$ vector of zero elements, and L is the length of zero-padding. We assume that the unknown discrete-time baseband CIR represents a multipath channel which introduces frequency-dependent Doppler effect. The latter is commonly compensated in the receiver using a packet preamble which is used for estimation and rescaling of the time axis [17]. Hereon, we look at the OFDM blocks after this compensation, which means that we deal with a multipath channel described by the $L \times 1$ vector

$$\mathbf{h} = [h(0), h(1), \dots, h(L - 1)]^T, \quad (4)$$

where L is the delay spread of the channel normalized by the sampling interval,¹ $T_s = T/K$. It is assumed that the $P \times 1$ received vector $\mathbf{y} = [y(0), \dots, y(P - 1)]^T$ may still consist of a frequency independent residual Doppler shift component which has the following structure [3,17]

$$\mathbf{y} = \mathbf{y}_0 + \mathbf{n} = \Gamma_P(\epsilon_0)\mathbf{H}\mathbf{u} + \mathbf{n}, \quad (5)$$

¹ In practice, prior measurements indicate the delay spread of the channel and we can set the CIR length to L . We assume that the channel length L is selected such that $L \leq Q \leq 2K + 1$. Actually, it should even hold for $1 < Q \ll K$. Thus, to avoid inter-block interference, we set the zero padding length equal to the channel length.

where \mathbf{y}_0 is the noise-free received signal, \mathbf{H} is a $P \times P$ Toeplitz matrix with first column and first row given by $[\mathbf{h}^T, \mathbf{0}_{P-L}^T]^T$ and $[h(0), \mathbf{0}_{P-1}^T]^T$, respectively, $\mathbf{n} = [n(0), n(1), \dots, n(P-1)]^T$ is a $P \times 1$ vector representing the additive noise, which we assume is modeled as a zero-mean circular complex white Gaussian with covariance matrix $\sigma_n^2 \mathbf{I}_P$. Also, we define the normalized CFO, ϵ_0 as the physical frequency offset relative to the carrier spacing, Δf . Accordingly, the $P \times P$ matrix $\Gamma_P(\epsilon_0)$ is defined as

$$\Gamma_P(\epsilon_0) = \text{diag}(1, e^{j2\pi \frac{\epsilon_0}{K}}, \dots, e^{j2\pi \frac{\epsilon_0}{K} (P-1)}). \quad (6)$$

Notice that in this formulation, the CFO is assumed to be constant. In practice, this approximation may not hold, thus the formulation will include $\epsilon[n]$, $n = 0, \dots, P-1$ instead of ϵ_0 .

3. Analysis of EVD-based CFO estimation

A group of low-complexity closed-form CFO estimators has been proposed in Amar et al. [23], Avrashi et al. [24]. Although showing some promising results, these methods suffer from two drawbacks, making them impractical: (a) They introduce high PAPR, and (b) they require a time-constant frequency offset. As background, we briefly repeat and analyze the results presented in Amar et al. [23] for the eigenvalue decomposition (EVD) based estimator.

First, the following observation is made: the transmitted time-domain signal can be decomposed into a known pilot tone and unknown data tone signals,

$$x(n) = \underbrace{\sum_{k \in S_p} \frac{1}{\sqrt{K}} s(k) e^{j \frac{2\pi}{K} nk}}_{\triangleq s_p(n)} + \underbrace{\sum_{k \in S_D} \frac{1}{\sqrt{K}} s(k) e^{j \frac{2\pi}{K} nk}}_{\triangleq \eta(n)}, \quad (7)$$

where $|s(k)| = 1$, and S_p, S_D are the index sets of the pilot and data tones, respectively. For equi-spaced pilots, $S_p = \{k : k \bmod G = 0\}$ and the samples of the time-domain signal associated with the pilot tones are

$$\tilde{s}_p(n) = \sum_{q=0}^{Q-1} \frac{1}{\sqrt{K}} s(qG) e^{j \frac{2\pi}{Q} nq}, \quad (8)$$

which is a Q -periodic signal. The random data related signal, $\eta(n)$, is treated as noise. It has been shown [23] that for $K \gg Q$ it is distributed as white Gaussian noise with $\eta(n) \sim \mathcal{N}(0, \frac{K-Q}{K})$. At this point, the OFDM signal, $x(n)$, is segmented into G segments of Q samples. Notice that the pilot signal is correlated while the so-called data originated noise is uncorrelated between any two segments. By using this feature of the signal, the commonly used estimator can be applied, where a repeated signal is correlated in order to estimate the frequency offset [26].

In [23] it has been proposed to use the constant pilot tone, $s(qG) = e^{j\phi_0}$, where ϕ_0 is some real number, to obtain

$$\begin{aligned} x(n) &= \sum_{q=0}^{Q-1} \frac{1}{\sqrt{K}} e^{j\phi_0} e^{j \frac{2\pi}{Q} nq} + \eta(n) \\ &= \frac{Q e^{j\phi_0}}{\sqrt{K}} \delta[n \bmod Q] + \eta(n) \end{aligned} \quad (9)$$

for $n = 0, \dots, K-1$. where

$$\delta[n] = \begin{cases} 1, & n = 1, \\ 0, & \text{otherwise.} \end{cases} \quad (10)$$

Here, we introduce the following assumption: The system design guarantees that there is no pilot signal leakage from one section to the consecutive, in the constant pilot tone setup, this translates to $L+1 < Q$. Specifically, it is guaranteed that the ZP section, $\mathbf{y}(K : K+P)$, holds only data-signal paths with no pilot remains. As the

CFO estimator treats the data signal as noise, it is beneficial, for this purpose only, to discard the ZP section. Therefore, instead of conducting the standard overlap-and-add operation for ZP-OFDM [3], we simply use the first K taps given by

$$\begin{aligned} \tilde{\mathbf{y}} &= \mathbf{T}_K \mathbf{y} \\ &= \mathbf{T}_K (\Gamma_P(\epsilon_0) \mathbf{H} \mathbf{u} + \mathbf{n}) \\ &= [\Gamma_K(\epsilon_0), \mathbf{0}_K \mathbf{0}_L^T] \mathbf{H} \mathbf{u} + \mathbf{T}_K \mathbf{n} \\ &= \Gamma_K(\epsilon_0) \mathbf{T}_K \mathbf{H} \mathbf{u} + \mathbf{T}_K \mathbf{n} \\ &= \Gamma_K(\epsilon_0) \mathbf{H}(1 : K, :) \mathbf{u} + \mathbf{T}_K \mathbf{n} \end{aligned} \quad (11)$$

instead of (5), where the trimming $K \times (K+L)$ matrix \mathbf{T}_K is defined as

$$\mathbf{T}_K = [\mathbf{I}_K, \mathbf{0}_K \mathbf{0}_L^T]. \quad (12)$$

The received OFDM signal is CFO compensated by pre-multiplying it by $\Gamma_K^H(\epsilon)$ for the hypothesized offset ϵ . The compensated block is then transformed to the frequency domain where the pilot carriers are extracted to obtain the $Q \times 1$ hypothesized output vector

$$\begin{aligned} \mathbf{x}(\epsilon) &= \mathbf{T}_{sc} \mathbf{F}_K \Gamma_K^H(\epsilon) \tilde{\mathbf{y}} \\ &= \mathbf{T}_{sc} \mathbf{F}_K \Gamma_K^H(\epsilon) \Gamma_K(\epsilon_0) \mathbf{T}_K \mathbf{H} \mathbf{u} + \eta \end{aligned} \quad (13)$$

where $\mathbf{T}_{sc} = \mathbf{I}_K(1 : G : K, :)$ selects the pilot tones and $\eta = \mathbf{T}_{sc} \mathbf{F}_K \Gamma_K^H(\epsilon) \mathbf{T}_K \mathbf{n}$ is a zero mean WGN. Substituting (5) into (13) when $\epsilon \cong \epsilon_0$ (meaning that the hypothesized and true offsets are close) implies that $\mathbf{x}(\epsilon)$ can be approximated as (see Appendix B)

$$\mathbf{x}(\epsilon) \cong \sqrt{Q} \mathbf{D}_p \mathbf{F}_Q(:, 1 : L) \mathbf{h} + \eta, \quad (14)$$

where \mathbf{h} is the $L \times 1$ CIR, \mathbf{D}_p is a $Q \times Q$ diagonal matrix containing the pilot symbols on its diagonal, $\mathbf{F}_Q(:, 1 : L)$ is obtained by taking the first L columns of the $Q \times Q$ Fourier transform matrix. In order to determine ϵ and \mathbf{h} , a nonlinear least squares (NLS) optimization problem is defined, where the estimated values minimize the Euclidean squared distance between $\mathbf{x}(\epsilon)$ and its approximation in (14), i.e.,

$$L(\epsilon, \mathbf{h}) = \|\mathbf{x}(\epsilon) - \sqrt{Q} \mathbf{D}_p \mathbf{F}_Q(:, 1 : L) \mathbf{h}\|^2. \quad (15)$$

Taking the derivative of (15) w.r.t. \mathbf{h} and equating the result to zero, yields the LS estimate of the channel response:

$$\hat{\mathbf{h}} = \frac{1}{\sqrt{Q}} \mathbf{F}_Q^H(:, 1 : L) \mathbf{D}_p^H \mathbf{x}(\epsilon), \quad (16)$$

Substituting (16) into (15) implies that the estimate of the CFO is obtained by selecting ϵ that minimizes the quadratic form

$$\begin{aligned} \ell(\epsilon) &= \mathbf{x}^H(\epsilon) \mathbf{D}_p [\mathbf{I}_Q - \mathbf{F}_Q(:, 1 : L) \mathbf{F}_Q^H(:, 1 : L)] \\ &\quad \times \mathbf{D}_p^H \mathbf{x}(\epsilon). \end{aligned} \quad (17)$$

It has been shown that $\mathbf{x}(\epsilon)$ can be expressed using a segmented version of the received signal given as

$$\mathbf{Y} = [\mathbf{y}(1 : Q), \dots, \mathbf{y}(K - Q + 1 : K)], \quad (18)$$

which means that \mathbf{Y} is a $Q \times G$ matrix obtained by arranging the Q -samples segments of \mathbf{y} in its columns. Using this formulation, (13) becomes

$$\mathbf{x}(\epsilon) = \mathbf{F}_Q \Gamma_Q^H(\epsilon) \mathbf{Y} \alpha(\epsilon), \quad (19)$$

where \mathbf{F}_Q is the $Q \times Q$ Fourier transform matrix, $\Gamma_Q(\epsilon) = \text{diag}(1, e^{j \frac{2\pi \epsilon}{Q}}, \dots, e^{j \frac{2\pi \epsilon}{Q} (Q-1)})$, and

$$\alpha(\epsilon) = [1, \dots, e^{-j \frac{2\pi \epsilon}{Q} (G-1)}]^T \quad (20)$$

is a $G \times 1$ vector holding the phase accumulations between the different segments such that $\Gamma_K(\epsilon) = \text{diag}\{\alpha^H(\epsilon)\} \otimes \Gamma_Q(\epsilon)$ where \otimes

is the Kronecker product. By replacing (19) into (17), the following form is obtained

$$\ell(\epsilon) = \|\mathbf{Y}\alpha(\epsilon)\|^2 - \|\mathbf{F}_Q^H(:, 1:L)\mathbf{D}_p^H\mathbf{F}_Q\Gamma_Q^H(\epsilon)\mathbf{Y}\alpha(\epsilon)\|^2. \quad (21)$$

It has been shown [24] (and see generalized analysis in Section 3.1) that by using identical pilot tones, (21) simplifies to the following cost function

$$\ell(\epsilon) = \|\mathbf{Y}(L+1:Q, :)\alpha(\epsilon)\|^2. \quad (22)$$

The EVD-based estimate consists of two steps. First, from (5) and the definition of \mathbf{Y} in (18), the following is obtained

$$\mathbf{Y}(L+1:Q, :) = \mathbf{Y}_0 + \mathbf{N}, \quad (23)$$

where \mathbf{Y}_0 and \mathbf{N} are defined similar to \mathbf{Y} for the vectors \mathbf{y}_0 , \mathbf{n} and then truncated to their last $Q-L$ rows. We assume that the noise-free part \mathbf{Y}_0 obtained from \mathbf{y}_0 (see (5)) is uncorrelated with the noise part, \mathbf{N} (obtained from \mathbf{n} in (5)). This assumption holds as it is reasonable to assume that the transmitted symbol vector, \mathbf{s} , is uncorrelated with the additive noise, \mathbf{n} . Substituting (23) into (22) and unfolding the norm yields

$$\ell_1(\epsilon) = \alpha^H(\epsilon) \left[\underbrace{\mathbf{Y}_0^H \mathbf{Y}_0}_{\mathbf{R}_0} + \mathbf{N}^H \mathbf{N} \right] \alpha(\epsilon). \quad (24)$$

Since $\mathbf{N}^H \mathbf{N}$ describes the covariance matrix of a white Gaussian noise with variance σ_n^2 , the cost function becomes²

$$\ell_1(\epsilon) = \alpha(\epsilon)^H \left[\underbrace{\mathbf{R}_0 + \sigma_n^2 \mathbf{I}_G}_{\hat{\mathbf{R}}} \right] \alpha(\epsilon). \quad (25)$$

Obviously, using \mathbf{R}_0 in place of $\hat{\mathbf{R}}$ in (25) yields that $\ell_1(\epsilon) = 0$ for $\alpha(\epsilon) = \alpha(\epsilon_0)$. This means that $\alpha(\epsilon_0)$ is an eigenvector of \mathbf{R}_0 corresponding to the zero eigenvalue. In [23] it is proven that this is the minimal eigenvalue of \mathbf{R}_0 with probability one. Consequentially, the minimal eigenvalue of $\hat{\mathbf{R}}$ is σ_n^2 and the following relation between the eigenvectors exists,

$$\mathbf{u}_{\min}(\hat{\mathbf{R}}) \cong \mathbf{u}_{\min}(\mathbf{R}_0) + \delta \mathbf{u}_{\min}, \quad (26)$$

where $\mathbf{u}_{\min}(\mathbf{A})$ is the eigenvector of the matrix \mathbf{A} corresponding to the smallest eigenvalue. Also, $\delta \mathbf{u}_{\min}$ is a small perturbation with zero mean. Since for the noiseless version \mathbf{R}_0 the minimal eigenvalue is simply $\alpha(\epsilon_0)$, a closed form estimate will be

$$\hat{\alpha}(\epsilon_0) = \mathbf{u}_{\min}(\hat{\mathbf{R}}) - \delta \mathbf{u}_{\min}. \quad (27)$$

The second step of the EVD estimation will be extracting the CFO ϵ_0 . This is done by observing the phase of (27) given by

$$-\frac{2\pi}{G} \mathbf{g}\epsilon_0 \cong \arg(\mathbf{u}_{\min}(\hat{\mathbf{R}})) - \arg(\delta \mathbf{u}_{\min}), \quad (28)$$

where $\mathbf{g} = [0, 1, \dots, G-1]^T$. Finally, the closed form estimate is given by the least squares (LS) solution of the problem formulated in (28),

$$\hat{\epsilon} = -\frac{G}{2\pi} \cdot \frac{\sum_{g=0}^{G-1} \mathbf{g}[\arg(\mathbf{u}_{\min}(\hat{\mathbf{R}}))]_g}{\sum_{g=0}^{G-1} g^2}. \quad (29)$$

This result requires an EVD of a $G \times G$ matrix followed by a simple linear combination of a $G \times 1$ vector. The result is a constant CFO value, assuming that it holds for the complete duration of the OFDM block. In other words, this solution assumes that the CFO is time-invariant during the OFDM block. In practical underwater acoustic channels, this may not hold.

² An intuitive approach to the described EVD based CFO estimate comes from the field of sensor array processing. We can consider ϵ as the direction of an arrival of the desired signal, and $\alpha(\epsilon)$ as a steering vector. The EVD solution is then analogous to a minimum variance beamformer.

3.1. Cost function analysis

Notice that the term

$$\mathbf{F}_Q^H(:, 1:L)\mathbf{D}_p^H\mathbf{F}_Q\Gamma_Q^H(\epsilon)\mathbf{Y}\alpha(\epsilon)$$

in (21) describes the L -tap cross correlation between the pilot signal and the CFO compensated sections. In order to better reflect this observation, we define the pilot-signal cross-correlation operator

$$\Psi = \mathbf{F}_Q^H\mathbf{D}_p\mathbf{F}_Q(:, 1:L), \quad (30)$$

which is a circulant matrix with the first column and first row given by $\psi = \text{IFFT}\{\text{diag}(\mathbf{D}_p)\}$ (the time domain pilot signal) and $[\psi(0), \dots, \psi(Q-L+1)]$, respectively (see Appendix A). The cost function in (21) then becomes

$$\ell(\epsilon) = \|\mathbf{Y}\alpha(\epsilon)\|^2 - \alpha^H(\epsilon)\mathbf{Y}^H\Gamma_Q(\epsilon)\Psi\Psi^H\Gamma_Q^H(\epsilon)\mathbf{Y}\alpha(\epsilon). \quad (31)$$

The matrix $\Psi\Psi^H$ in (31) has the following structure: Consider the top-left block matrix with size $\max(L+L_p-1, Q) \times \max(L+L_p-1, Q)$ block is defined similarly to \mathbf{r}_ψ , the cyclic autocorrelation function of ψ , where L_p is the support of ψ . The remaining entries of the matrix are equal to zero. Fig. 1 illustrates the diagonal and off-diagonal of $\Psi\Psi^H$ for a few important examples. It can be observed that for identical pilot tones, the pilot signal is a complex Delta function, which means that $L_p = 1$ and the autocorrelation is a real Delta function, resulting in the structure,

$$\Psi\Psi^H = \begin{bmatrix} \mathbf{I}_L & \mathbf{0}_{L \times (Q-L)} \\ \mathbf{0}_{(Q-L) \times L} & \mathbf{0}_{(Q-L) \times (Q-L)} \end{bmatrix}. \quad (32)$$

Substituting (32) into (31) yields the previous result (22), which significantly reduces the dimension of the problem from Q to G (notice that the term in (22) is a G -order polynomial). When $L_p > 1$, the structure of $\Psi\Psi^H$ is affected. As can be seen in Fig. 1, the non-zero block is contaminated by edge effects. These $(L_p-1) \times (L_p-1)$ sub-blocks in the top-left and bottom-right are a result of cyclic cross correlation of a zero-padded signal. The resulting cost function is

$$\ell(\epsilon) = \|\mathbf{Y}(L+L_p:Q, :)\alpha(\epsilon)\|^2 + r_{L_p}(\epsilon), \quad (33)$$

where $r_{L_p}(\epsilon)$ is the cost function residual caused by the two $(L_p-1) \times (L_p-1)$ sub-blocks of $\Psi\Psi^H$. It is clear that as we increase L_p , the larger the residual, up to a point where it completely dominates the cost function. This happens when $L_p > Q-L$, as in the case of random pilots. In this case $\ell(\epsilon) = r_Q(\epsilon)$ and a grid search should be performed [17]. For the rest of our analysis we assume that L_p is chosen such that $r_{L_p}(\epsilon) \ll \|\mathbf{Y}(L+L_p:Q, :)\alpha(\epsilon)\|^2$ and thus ignored, resulting in the approximated cost function,

$$\ell_1(\epsilon) \cong \|\mathbf{Y}(L+L_p:Q, :)\alpha(\epsilon)\|^2. \quad (34)$$

Similarly to the identical-pilot design, the cost function in (34) enables a closed form solution. In the next sections we will utilize the generalization from $L_p = 1$ to a carefully designed L_p in order to control the resulting PAPR.

3.2. Time locality - PAPR tradeoff in pilot tone design

The key to the closed-form CFO estimator is having an OFDM block with alternating sections of pilot signal and absence of it. In other words, we want to design our pilot tones such that the corresponding time domain signal will have a localized envelope, while having unit amplitude and equi-spaced pilots which maintain a simple channel equalizer [17]. In order to compare the time locality feature of different candidate pilot signals, we introduce the pilot-to-data ratio (PDR), describing the power ratios in the

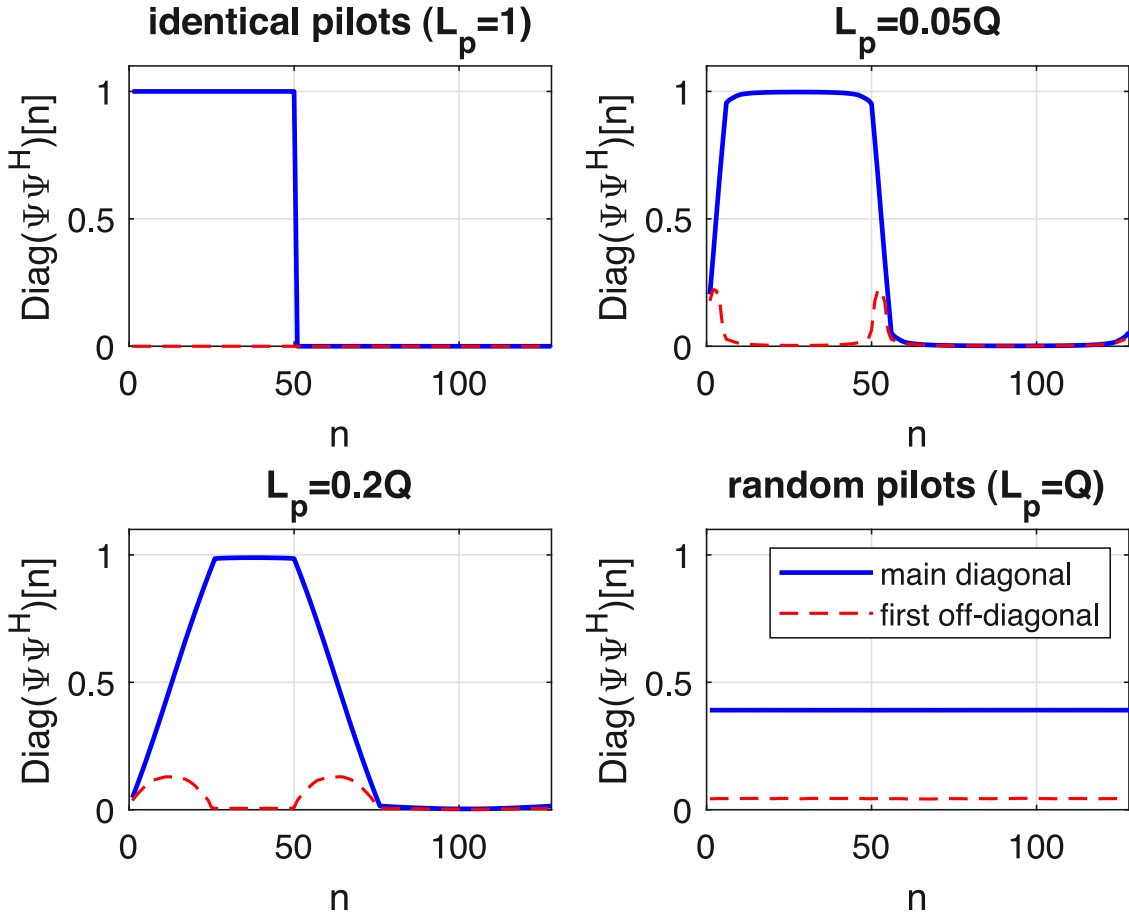


Fig. 1. Examples of the diagonals of $\Psi\Psi^H$ for 4 different L_p values where $Q = 128$ and $L = 50$. The main diagonals are compared to the first off-diagonal.

non-zero areas of the pilot signal. For a L_p support pilot signal, the PDR is given by

$$\begin{aligned} \text{PDR} &= \frac{\frac{1}{L_p} \sum_{n=1}^{L_p} |s_p(n)|^2}{\sigma_\eta^2} \\ &= \frac{\frac{K}{L_p} \sum_{n=1}^{L_p} |s_p(n)|^2}{K - Q}. \end{aligned} \quad (35)$$

The most trivial and effective pilot design, which meets the requirements is the identical-tone described in (9), where $L_p = 1$ and the PDR is $\frac{Q^2}{K-Q}$. Although optimal in terms of time locality, the identical pilot approach causes high PAPR. This is simply due to the contradicting requirements, that while trying to concentrate the time domain pilot signal, we incidentally cause high PAPR. From (9) we see that by selecting identical pilots we obtain a peak value of $\max |s_p(n)| = \frac{Q}{\sqrt{K}}$, therefore the expected value of PAPR is

$$\begin{aligned} E[\text{PAPR}] &= E \left[\frac{\max |x(n)|^2}{\frac{1}{K} \sum_{n=1}^K |x(n)|^2} \right] \\ &\cong \left(\frac{Q}{\sqrt{K}} + \sqrt{\frac{K-Q}{K}} \right)^2. \end{aligned} \quad (36)$$

In Fig. 2 we show two transmitted signals for $G = 4$ and $G = 8$. Expectedly from (36), as we decrease G , i.e., increase Q , the peak values increase.

In the next sections we offer a complete workframe that allows tackling and compromising between the two profound problems of the current closed-form CFO estimators: (1) In the transmitter side, designing the pilot tones that will allow closed form estimation

while causing negligible PAPR increase; (2) designing receiver algorithm that can handle time-varying CFO. Our ultimate goal is to decode the data symbols vector \mathbf{s} given that the normalized time-varying CFO, $\epsilon[n]$, and the CIR, \mathbf{h} , are unknown. For simplicity, we assume a constant CFO in the following section.

4. A constrained optimization for pilots design

In order to overcome the increase in PAPR, we propose to redesign the pilot tones in a way that both requirements are met: Localized pilot signal along with reasonably low PAPR. Notice, that unlike classical PAPR reduction schemes, which attempts to reduce the PAPR for the complete block, here we concentrate on reducing the PAPR caused by the pilot-tones in a limited number of taps determined by the CFO estimation algorithm. We start by looking for time domain pilot signals which will allow a compromise between these two contradicting requirements. While identical pilots are highly localized with the worst PAPR, random pilots will have the best PAPR and worst time locality. It is thus suggested to use a windowed envelope for the time domain signal. This window is expressed by $w = [w_1, w_2, \dots, w_{L_p}, 0, \dots, 0]^T$ (we selected a standard rectangular window, while other windows can be employed as well). Ideally, the first L_p taps of the signal will contain all the pilot energy. Note that L_p should be chosen such that $L_p + L < Q$.

The problem we turn to solve now can be defined as follows: We have pilot tones with known unit amplitudes and an unknown phase, denoted by $e^{j\phi}$, and the corresponding time domain signal is constrained by the windowed envelope. This is known as a phase retrieval problem, which has been studied in the past few decades in various fields. The problem was first addressed by Ger-

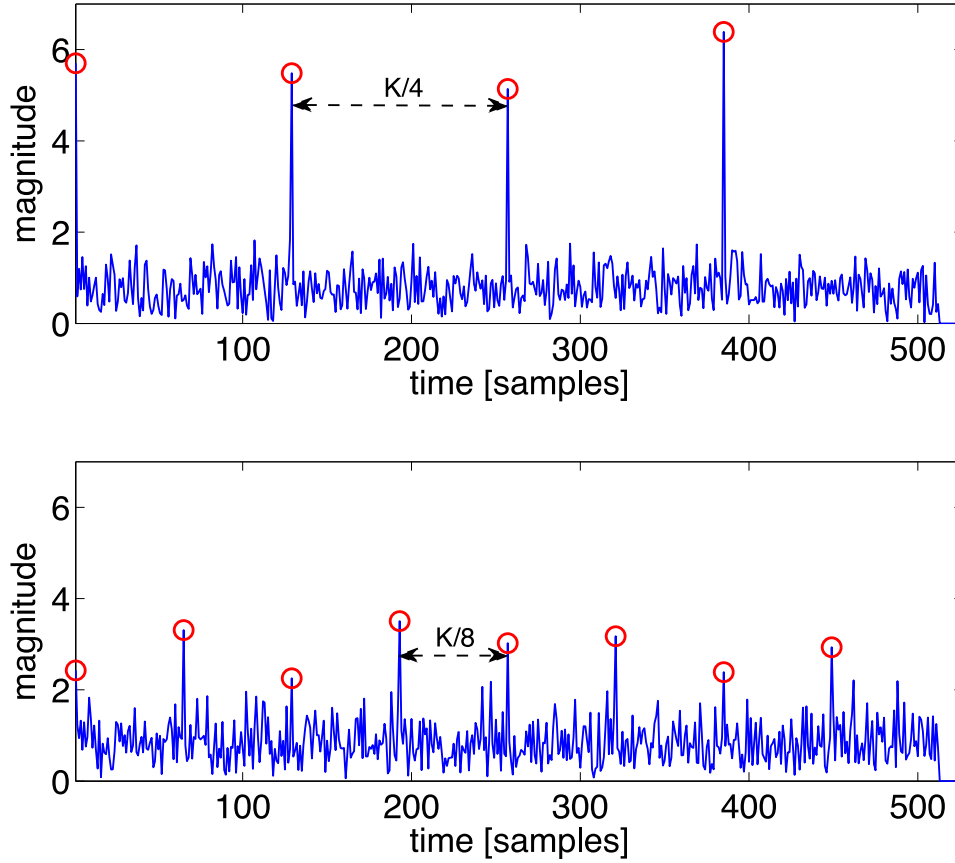


Fig. 2. Examples of the discrete time OFDM block ($G = 4$ for the upper plot, and $G = 8$ for the bottom plot).

chberg and Saxton [29] and later on by Fienup [30], who offered a set of algorithms for solving the problem of recovering a complex image from the measured magnitudes of a real image and far-field Fourier plane in optics. More recently, phase retrieval was suggested for optical imaging [32]. In [31], a pilot tone phase retrieval in OFDM communications was proposed for the receiver side, allowing the transmitter to choose the pilot phases without informing the receiver. Here we use a generalization of the Gerchberg-Saxton algorithm (GSA), called the error reduction algorithm [33], to reconstruct the pilot phases in the transmitter side.

Given the pilot tones in the frequency domain, $e^{j\phi}$ (at the initialization step, these phases are selected at random) and the desired pilot time domain signal \mathbf{s}_p , the problem can be formulated as

$$\begin{aligned} \min_{\phi} \quad & \|\mathbf{s}_p - F_Q^H e^{j\phi}\|^2 \\ \text{s.t.} \quad & s_p(n) = 0, \text{ for } n = L_p + 1, \dots, Q. \end{aligned} \quad (37)$$

The error reduction algorithm solves this non-convex problem iteratively by alternating projections. The algorithm transforms the time and frequency domain signals back and forth, where in each such alternation the amplitude constraint is applied (see Algorithm 1). Note that the end condition employs the error magnitude of the time domain constraint, but one may consider other criteria, such as a weighted sum of the achieved PAPR and time domain error. An example of the resulting OFDM block using a rectangular window is presented in Fig. 3. Here we used $K = 512$ subcarriers, the pilot spacing is $G = 4$ and L_p is chosen to be 10% of the pilot signal period, Q . In this example, the resulting PAPR was

Algorithm 1 Constrained pilots design.

```

1: define  $\mathbf{W} = \text{diag}[w_1, \dots, w_{L_p}, 0, \dots, 0]$ 
2: initialize  $\phi_0, \varepsilon = \infty, \mathbf{a}_0 = \text{IFFT}(e^{j\phi_0})$ 
3: while  $\varepsilon > \eta$  do
4:    $\mathbf{b}_i = \exp\{j \arg[\mathbf{a}_{i-1}]\}$ 
5:    $\mathbf{c}_i = \text{FFT}(\mathbf{W}\mathbf{b}_i)$  ▷ Applying time domain constraint
6:    $\mathbf{d}_i = \exp\{j \arg[\mathbf{c}_i]\}$ 
7:    $\mathbf{a}_i = \text{IFFT}(\mathbf{d}_i)$ 
8:    $\varepsilon = \|\mathbf{a}_i[L_p + 1, \dots, Q]\|^2$ 
9: end while
10: return  $\mathbf{d}_i$ 

```

10 dB, compared to the identical pilot waveform which results in an expected PAPR of 16.3 dB.

At this point, we have designed the transmitted waveform, which allows us to use low complexity CFO estimators while controlling the PAPR values. We now turn to design the receiver side CFO estimator.

5. Time varying CFO estimation

OFDM waveforms are commonly designed such that one block duration is shorter than the coherence time of the channel [20]. However, the coherence time may vary between different environments and sea states in such a way that enforcing the block duration to be shorter may cause significant loss of bit rate. In this section, we extend our closed-form CFO estimate to a time-varying model.

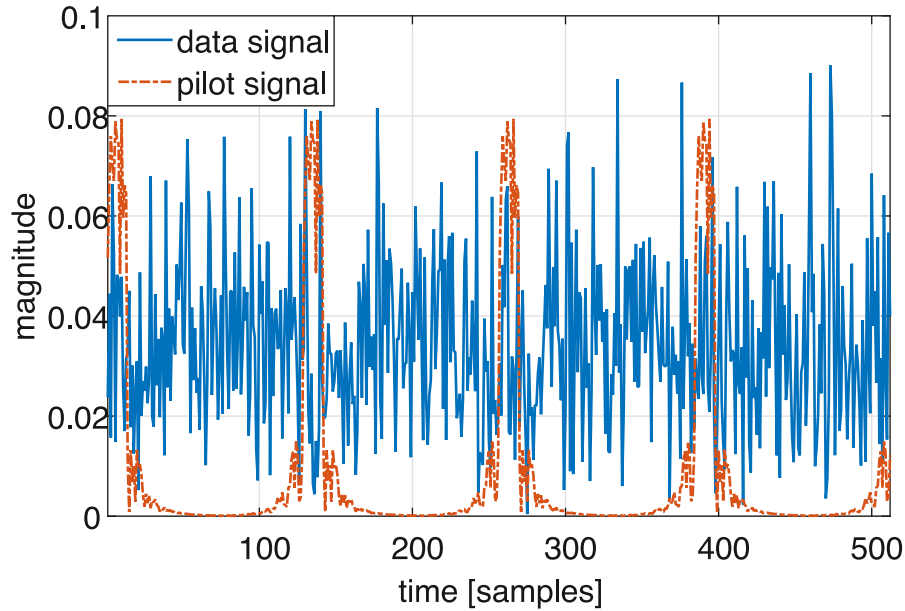


Fig. 3. Examples of the discrete time OFDM block with $G = 4$ where the pilot tones are designed with the phase retrieval algorithm for $L_p = 0.1Q$.

5.1. Polynomial model

Let us assume that the CFO is some continuous function in time, and that it can be represented by its Taylor polynomial

$$\epsilon[n] = \sum_{l=0}^{\infty} \epsilon_l^n, \quad 0 \leq n \leq K-1. \quad (38)$$

Substituting (38) into (6) we obtain

$$\Gamma_p = \text{diag} \left\{ 1, \exp \left[\frac{j2\pi}{K} \sum_{l=0}^{\infty} \epsilon_l \right], \dots, \exp \left[\frac{j2\pi}{K} (P-1) \sum_{l=0}^{\infty} \epsilon_l (P-1)^l \right] \right\}. \quad (39)$$

The received signal is defined similarly to (5), where Γ_p is determined by a time varying CFO,

$$\mathbf{y} = \Gamma_p \mathbf{H} \mathbf{T}_{zp} \mathbf{F}_K^H \mathbf{s} + \mathbf{n}. \quad (40)$$

We now turn to apply the EVD solution to the time-varying model. First, we notice that $\hat{\mathbf{R}}$ in (25) represents the correlation matrix of the G OFDM segments and thus inherent in this solution. Therefore, we turn to look at the g th section of \mathbf{y} , denoted by $\mathbf{y}_g = \Gamma_g \mathbf{z}_g + \mathbf{n}_g$, where \mathbf{z}_g is the CFO compensated signal obtained by taking the Q samples of the g th section of $\mathbf{H} \mathbf{T}_{zp} \mathbf{F}_K^H \mathbf{s}$, and

$$\Gamma_g = \text{diag} \left\{ \exp \left[\frac{j2\pi}{K} \sum_{l=0}^{\infty} (gQ)^{l+1} \epsilon_l \right], \dots, \exp \left[\frac{j2\pi}{K} \sum_{l=0}^{\infty} (gQ + Q - 1)^{l+1} \epsilon_l \right] \right\}. \quad (41)$$

Notice that last L taps of \mathbf{y} are discarded since it has no contribution to the CFO estimation as we assume that $L + L_p < Q$. The correlation of any two sections g and g' will give the following expression,

$$\mathbf{y}_g^H \mathbf{y}_{g'} = \mathbf{z}_g^H \Gamma_g^H \Gamma_{g'} \mathbf{z}_{g'} + \mathbf{n}_g^H \mathbf{n}_{g'}, \quad (42)$$

where the elements involving signal and noise products are assumed zero. Let us derive the CFO related term in (42),

$$d_{g,g'}[n] = \exp \left\{ \frac{j2\pi}{K} \sum_{l=0}^{\infty} \epsilon_l \left[(n + g'Q)^{l+1} - (n + gQ)^{l+1} \right] \right\} \quad (43)$$

where $d_{g,g'}[n] = \text{diag} \{ \Gamma_g^H \Gamma_{g'} \} [n]$. Notice that each binomial of the term can be represented as $(n + gQ)^l = (gQ)^l + n^l + r_l(n, g)$ where

$$r_l(n, g) = \sum_{k=1}^{l-1} \binom{l}{k} n^{l-k} (gQ)^k \quad (44)$$

is the residual of the binomial decomposition, for instance $r_0(n, g) = 0$, $r_1(n, g) = 0$, and $r_2(n, g) = 2ngQ$. Using this formulation we obtain

$$d_{g,g'}[n] = \underbrace{\exp \left\{ -\frac{j2\pi}{G} \sum_{l=1}^{\infty} g^l Q^{l-1} \epsilon_{l-1} \right\}}_{\alpha_g^*} \times \underbrace{\exp \left\{ \frac{j2\pi}{K} \sum_{l=1}^{\infty} \epsilon_l [r_l(n, g') - r_l(n, g)] \right\}}_{\lambda_{g,g'}[n]} \times \underbrace{\exp \left\{ \frac{j2\pi}{G} \sum_{l=1}^{\infty} g'^l Q^{l-1} \epsilon_{l-1} \right\}}_{\alpha_{g'}} \quad (45)$$

where α_g is the constant inter-section phase accumulation and $\lambda_{g,g'}[n]$ is the difference between phases accumulated within two sections. Next, (42) can be written as

$$\mathbf{y}_g^H \mathbf{y}_{g'} = \alpha_g^* \alpha_{g'} \mathbf{z}_g^H \Lambda_{g,g'} \mathbf{z}_{g'} + \mathbf{n}_g^H \mathbf{n}_{g'}, \quad (46)$$

where $\Lambda_{g,g'} = \text{diag} \{ \lambda_{g,g'}[0], \dots, \lambda_{g,g'}[Q-1] \}$. Ideally, the matrix $\Lambda_{g,g'}$ can be neglected. For zero-order and first-order polynomials, $\Lambda_{g,g'}$ is the identity matrix, in which case we obtain the cost function (17). However, as higher orders are introduced, the accumulated phase may not be negligible depending on ϵ_l and G . Therefore, we will omit $\Lambda_{g,g'}$ when the CFO function can be approximated as linear and the residual is kept small, otherwise it may

dominate the cost function. By using the above approximation, we obtain the EVD formulation for the polynomial time varying model.

$$\mathbf{y}_g^H \mathbf{y}_{g'} = \alpha_g^* \alpha_{g'} \mathbf{z}_g^H \mathbf{z}_{g'} + \mathbf{n}_g^H \mathbf{n}_{g'}. \quad (47)$$

Collecting all section correlations into the matrix

$$\mathbf{R}_{PL} = \mathbf{Y}^H \mathbf{Y}, \quad (48)$$

and substituting (48) into (34), we obtain the optimization problem

$$\operatorname{argmin}_{\alpha} \alpha^H \mathbf{R}_{PL} \alpha \quad \text{s.t.} \quad \alpha^H \alpha = G, \quad (49)$$

where we added the constraint on α in order to guarantee the structure in (20). Notice that $\alpha^H \alpha = G$ is a weak constraint, which is enough in order to define the equivalent optimization problem of minimizing the following Rayleigh quotient,

$$R(\mathbf{R}_{PL}, \alpha) = \frac{\alpha^H \mathbf{R}_{PL} \alpha}{\alpha^H \alpha}. \quad (50)$$

The quotient in (50) is minimized by the eigenvector corresponding to the smallest EV of \mathbf{R}_{PL} , yielding

$$\operatorname{arg}[\mathbf{u}_{\min}(\mathbf{R}_{PL})](g) = -\frac{2\pi}{G} \sum_{l=1}^{G-1} g^l Q^{l-1} \epsilon_{l-1} + v_g, \quad (51)$$

where v_g is assumed to be zero-mean Gaussian noise with unknown variance σ_v^2 . Converted to matrix formulation

$$\operatorname{arg}[\mathbf{u}_{\min}(\mathbf{R}_{PL})](g) = -\frac{2\pi}{G} \mathbf{a}_g^T \mathbf{Q} \epsilon + v_g, \quad (52)$$

where

$$\begin{aligned} \mathbf{a}_g &= [g, g^2, \dots, g^{G-1}]^T, \\ \mathbf{Q} &= \operatorname{diag}\{1, Q, \dots, Q^{G-2}\}, \\ \epsilon &= [\epsilon_0, \epsilon_1, \dots, \epsilon_{G-2}]^T. \end{aligned}$$

Collecting all G elements of α , we obtain

$$\mathbf{r} \equiv \operatorname{arg}[\mathbf{u}_{\min}(\mathbf{R}_{PL})] = -\frac{2\pi}{G} \mathbf{A} \mathbf{Q} \epsilon + \mathbf{v}, \quad (53)$$

where $\mathbf{A} = [\mathbf{a}_0, \dots, \mathbf{a}_{G-1}]^T$. Once again, as in the constant CFO case, the problem reduces to an LS formulation. As the elements of α represent the phase accumulated between the block sections due to CFO, we use it as a stepping stone towards reconstructing ϵ .

Given the measurement vector \mathbf{r} (obtained by the EVD estimator), the LS problem defined by the polynomial model is given by

$$\hat{\epsilon} = \operatorname{argmax}_{\epsilon} \left\| \mathbf{r} + \frac{2\pi}{G} \mathbf{A} \mathbf{Q} \epsilon \right\|^2. \quad (54)$$

The closed form solution is given by

$$\hat{\epsilon} = -\frac{G}{2\pi} \mathbf{Q}^{-1} (\mathbf{A}^T \mathbf{A})^{-1} \mathbf{A}^T \mathbf{r}. \quad (55)$$

Notice that due to the structure of \mathbf{A} , inverting $\mathbf{A}^T \mathbf{A}$ can be numerically challenging as its eigenvalues grow exponentially. In order to overcome this, we alternate our model by introducing the normalized coefficients $b_l = K^l \epsilon_l$. Since we assume $|\epsilon[n]| < 1$ (practically, it is sufficient to assume that the CFO is within the order of 1), then $b_l < 1$. Replacing the normalized coefficients into (53), we have

$$\mathbf{r} = -\frac{2\pi}{G} \underbrace{\mathbf{A} \mathbf{Q} \tilde{\mathbf{K}}}_{\tilde{\mathbf{A}}} \mathbf{b} + \mathbf{v}, \quad (56)$$

where $\mathbf{b} = [b_0, b_1, \dots, b_{G-1}]^T$ and $\tilde{\mathbf{K}} = \operatorname{diag}(K^0, K^{-1}, \dots, K^{-(G-1)})$. By introducing this model alternation, we obtain a more convenient matrix $\tilde{\mathbf{A}}$, defined by its (g, l) th element $\tilde{\mathbf{A}}_{g,l} = (\frac{g}{K})^l$. Using this formulation in the LS solution we have

$$\hat{\epsilon} = -\frac{G}{2\pi} \tilde{\mathbf{K}} (\tilde{\mathbf{A}}^T \tilde{\mathbf{A}})^{-1} \tilde{\mathbf{A}}^T \mathbf{r}. \quad (57)$$

5.2. Piecewise constant model

As mentioned, the main drawback of the polynomial approach is that it disregards the matrix $\Lambda_{g,g'}$, which incorporates the difference in inner-section phase accumulation of two different sections. Since this is not a constant function, it may introduce a non-negligible effect. Ideally the phase accumulated from one section to another is identical to all samples. Let us consider a piecewise constant model for the time varying CFO as follows,

$$\epsilon[n] = \sum_{g=0}^{G-1} \epsilon_g u_g[n], \quad (58)$$

where

$$u_g[n] = \begin{cases} 1, & gQ \leq n \leq (g+1)Q - 1, \\ 0, & \text{otherwise.} \end{cases} \quad (59)$$

Substituting (58) into (6), we obtain Γ_K with the received signal being $\mathbf{y} = \Gamma_K \mathbf{H} \mathbf{T}_{zp} \mathbf{F}_K^H \mathbf{s} + \mathbf{n}$. Following the same steps leading to (43), we obtain the CFO related term of the inter-section correlation,

$$\begin{aligned} d[n] &= \exp \left\{ \frac{j2\pi}{K} [\epsilon_{g'}(n + g'Q) - \epsilon_g(n + gQ)] \right\} \\ &= \underbrace{\exp \left\{ -\frac{j2\pi}{G} \epsilon_g g \right\}}_{\alpha_g^*} \underbrace{\exp \left\{ \frac{j2\pi}{K} (\epsilon_{g'} - \epsilon_g) n \right\}}_{\lambda_{g,g'}[n]} \alpha_{g'} \\ &\quad \times \underbrace{\exp \left\{ \frac{j2\pi}{G} \epsilon_{g'} g' \right\}}. \end{aligned} \quad (60)$$

Once again we encounter the inner-section phase accumulation difference (PAD), which can be at most $\frac{2\pi}{K} |\epsilon_{g'} - \epsilon_g| (Q - 1)$. The inter-section PAD, however, is at least $\frac{2\pi}{K} |\epsilon_{g'} - \epsilon_g| Q$. Here, we neglect the inner-section PAD. Notice that not correlating adjacent sections and/or trimming the end of each section will further weaken the effect of inner-section PAD. The EVD-estimator of the piecewise constant model yields

$$\operatorname{arg}[\mathbf{u}_{\min}(\mathbf{R}_{PWC})](g) = -\frac{2\pi}{G} \epsilon_g g + v_g. \quad (61)$$

Collecting all G elements of α we obtain

$$\mathbf{r} \equiv \operatorname{arg}[\mathbf{u}_{\min}(\mathbf{R}_{PL})] = -\frac{2\pi}{G} \mathbf{G} \epsilon + \mathbf{v}, \quad (62)$$

where $\mathbf{G} = \operatorname{diag}\{0, 1, \dots, G-1\}$ and $\epsilon = [\epsilon_0, \dots, \epsilon_{G-1}]^T$. The LS solution of (62) is

$$\hat{\epsilon} = -\frac{G}{2\pi} G^{-1} \mathbf{r}. \quad (63)$$

Notice that the vector \mathbf{r} collects all inter-section phase accumulations with an arbitrary initial phase. In order to achieve the PAD needed for the estimation, we need to shift the phase according to the first element (in other words taking the phase derivative). By doing so, we are left with zero in the first element of \mathbf{r} , meaning that ϵ_0 cannot be estimated. One can use the remaining $G-1$ non zero elements to estimate ϵ_0 with various methods. In our implementation, we choose to use the following weighted sum

$$\hat{\epsilon}_0 = \frac{\sum_{g=1}^{G-1} (G-g)^2 \hat{\epsilon}_g}{\sum_{g=1}^{G-1} g^2}, \quad (64)$$

which is essentially an extrapolation operation. Another possible approach is compensating for the $G-1$ estimated sections and then conducting a one-dimensional search for ϵ_0 .

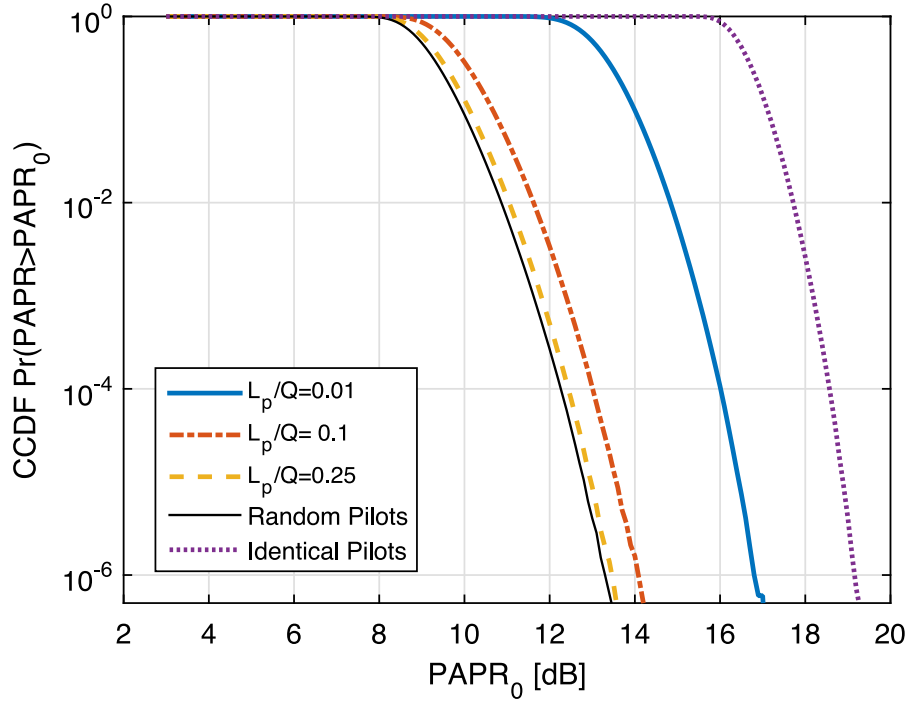


Fig. 4. CCDF of PAPR for different window sizes.

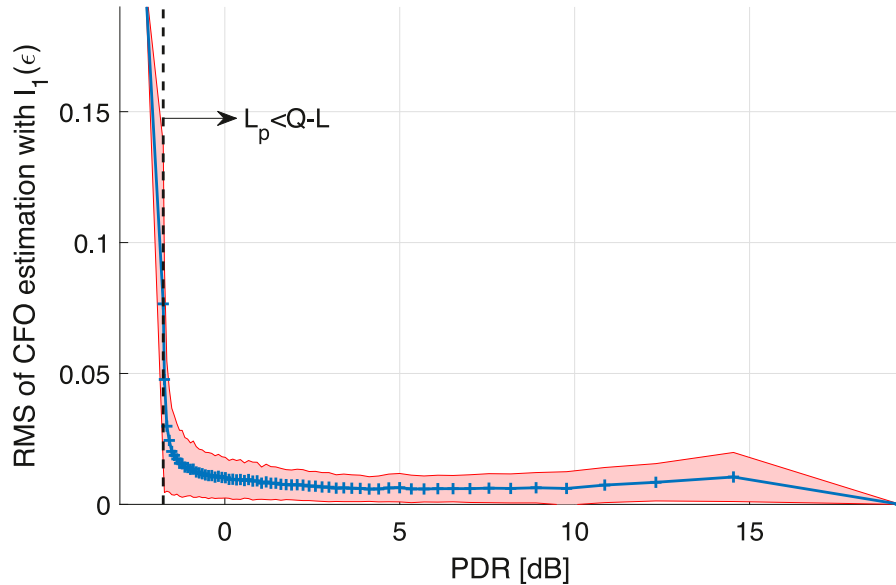


Fig. 5. Effect of the PDR on the cost function error. The horizontal axis describes the average PDR [dB] while the vertical corresponds to the RMS of the CFO error when using $\ell_1(\epsilon)$ with a grid search, the colored area represents the bounds of the estimation error. When L_p exceeds $Q - L$ (in this case $L = 0.5Q$), the cost function will not have a minimum, as a result, the minimum value will be one of the search grid bounds.

6. Simulations results

6.1. PAPR reduction

In this section, the reduced PAPR scheme is analyzed by simulations. Fig. 4 shows the PAPR complementary cumulative distribution function (CCDF). L_p values of 1%, 10% and 25% of the section length, $Q = 256$, are compared to the random and identical pilot cases. It can be seen that choosing a window of 10% results in a CCDF of merely 0.8 dB from the random pilots case. Depending on the expected channel delay spread, one can choose a window size which will compromise between the resulting PAPR, the channel

taps needed and the remaining so-called noise space taps, not affected by the pilots, defined as $L_\epsilon = Q - L_p - L + 1$.

6.2. CFO estimation as a function of PDR

In Section 3.2 we have discussed the tradeoff between the PDR and PAPR. While it is quite clear what are the implications of high PAPR, it is important to examine the PDR as well. Fig. 5 shows the effect of increasing PDR on the estimation error. Simulation is performed using $K = 1024$, $Q = 256$. It can be seen that for high PDR values the estimation error is reasonably small (0.6% of carrier spacing for PDR= 10 dB). However, when approaching $Q - L$,

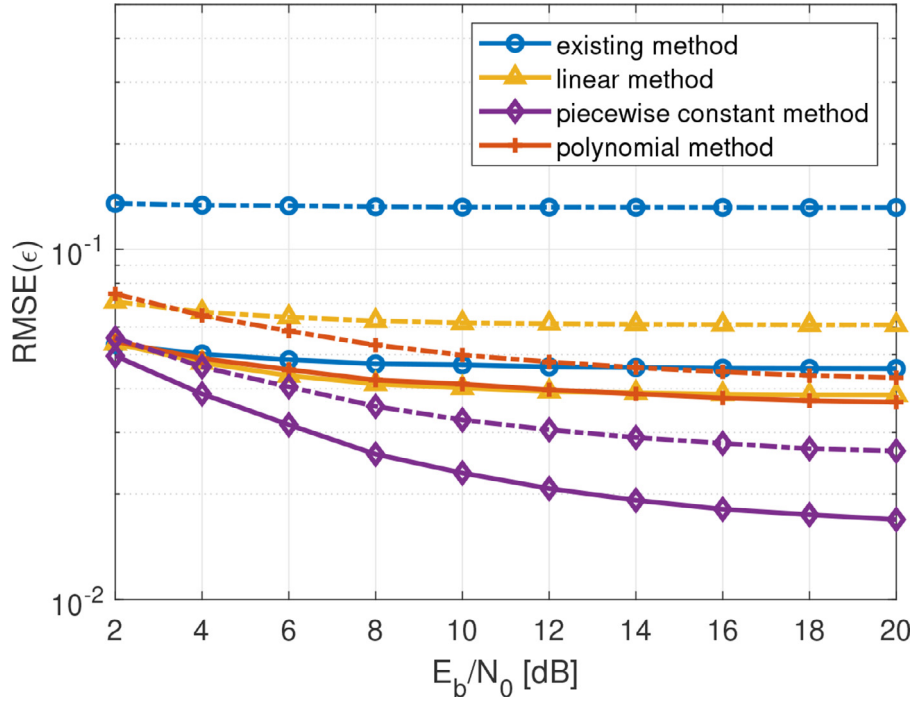


Fig. 6. RMSE of time-varying CFO estimators. Results for a sinusoidal time-variation are depicted in solid lines while dashed lines correspond to the polynomial time-variation.

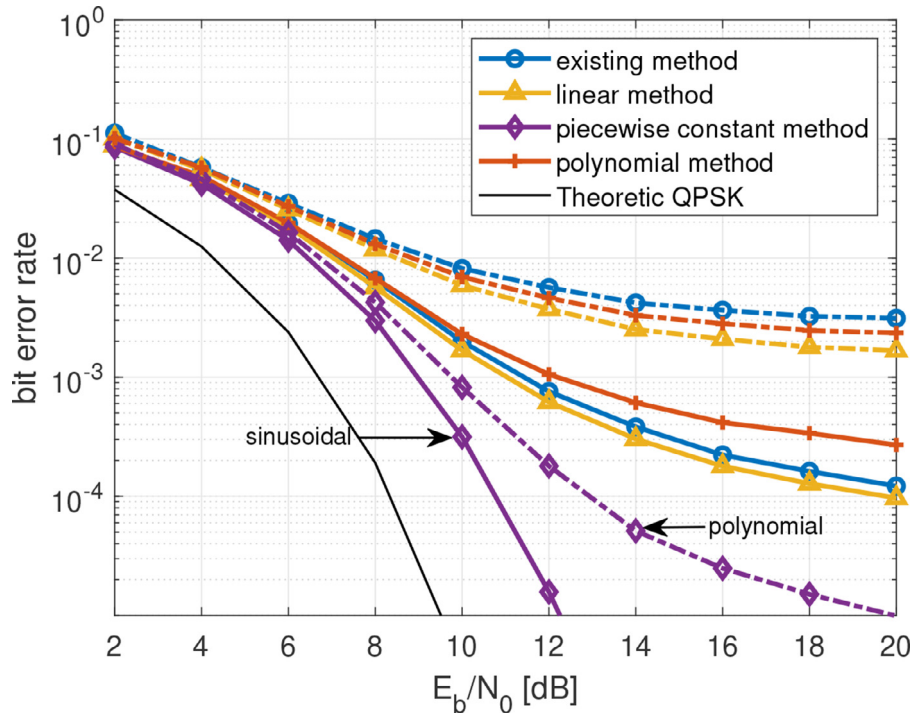


Fig. 7. Bit error rate of time-varying CFO estimators.

the error drastically increases. Interestingly, the generally monotonic curve in Fig. 5 has a peak at a very high PDR value. This is caused by the large error of Algorithm 1 when working with a very narrow window (in this case 2 and 3 taps).

6.3. Simulative CFO estimation results

We evaluate the performance of the proposed estimates using numerical simulations. We used OFDM blocks of $K = 2048$ QPSK

symbols with $G = 8$ and bandwidth of $W = K\Delta f = 12.5$ KHz. The simulated channel was produced using a geometrical model of a shallow water environment. The receiver and transmitter were located 2000 m apart at a depth of 5 m and 4 m, and the seabed to 70 m. The geometrical model included 10 paths with random phases [28]. The delay spread was set to 30 ms. Time-varying frequency offsets of two types were simulated: (1) polynomial time variation of order 4, where the coefficients were randomly drawn from the uniform distribution $b_l \sim \mathcal{U}[-0.25, 0.25]$; (2) sinusoidal

time variation of the form

$$\epsilon(n) = \Delta f \left[A_0 + A \sin(2\pi n \frac{f_{\sin}}{K}) \right], \quad (65)$$

where $A_0, A \sim \mathcal{U}[-0.25, 0.25]$ and $f_{\sin} \sim \mathcal{U}[0.25, 2]$. The time-varying and constant CFO estimators were simulated over the models and compared. Fig. 6 presents the root-mean-square error (RMSE) of CFO estimation versus the signal-to-noise ratio (SNR). The solid lines represent the results for the sinusoidal CFO, which in this case have lower error compared to the polynomial CFO, represented in dashed line. As can be seen, the piecewise-constant estimator's error is consistently lower than that of the linear estimator, which in turn, is lower than the previously published constant CFO estimator. However, the polynomial estimation model achieves inferior results, which in the sinusoidal case is even worse than the constant model. This is due to the approximation of (46) which apparently does not hold in this simulation. Fig. 7 shows how the CFO estimation error ultimately affects the bit error rate (BER) performance. What has appeared to be an incremental improvement in the CFO accuracy is translated to a significant improvement in the system performance, which in this case reached up to 9 dB for the sinusoidal CFO and a make-or-brake for the polynomial CFO.

7. Conclusions

We have presented a complete transmitter-receiver scheme for underwater acoustic communication with time-varying channels. We have expanded the previously suggested closed-form CFO estimator to handle the inherent drawback of high PAPR and included a model-based estimator for rapidly changing frequency offsets. The proposed framework enables full flexibility for the modem designer to compromise between the estimator performance and the PAPR reduction, such that it could be optimized for specific channels. The scheme can also be easily integrated into other multi-carrier modems where the medium characteristics dictate a fast varying channel and a limited bandwidth. Simulations show that the framework has significant contribution in lowering the PAPR, it also shows that assuming complex frequency variation models (starting from constant, through linear and piecewise linear) can be translated into BER reduction using the proposed method. Future research will focus on comparing the computational loads between the proposed design of the transmitted waveform and other waveform designs, further analyzing the feasibility of the proposed estimators in realistic time-varying channels, and sea trials shall be conducted in order to validate the proposed methods in real environments.

Declaration of Competing Interest

The authors declare that they have no known competing financial interests or personal relationships that could have appeared to influence the work reported in this paper.

Appendix A. Structure of Ψ

Consider the matrix Ψ in (30) which is expressed explicitly as

$$\Psi = \begin{bmatrix} \mathbf{F}_Q^H(:, 1) \mathbf{D}_p \mathbf{F}_Q^H(:, 1) & \dots & \mathbf{F}_Q^H(:, 1) \mathbf{D}_p \mathbf{F}_Q^H(:, L) \\ \mathbf{F}_Q^H(:, 2) \mathbf{D}_p \mathbf{F}_Q^H(:, 1) & \dots & \mathbf{F}_Q^H(:, 2) \mathbf{D}_p \mathbf{F}_Q^H(:, L) \\ \vdots & \dots & \vdots \\ \mathbf{F}_Q^H(:, L) \mathbf{D}_p \mathbf{F}_Q^H(:, 1) & \dots & \mathbf{F}_Q^H(:, L) \mathbf{D}_p \mathbf{F}_Q^H(:, L) \\ \vdots & \dots & \vdots \\ \mathbf{F}_Q^H(:, Q) \mathbf{D}_p \mathbf{F}_Q^H(:, 1) & \dots & \mathbf{F}_Q^H(:, Q) \mathbf{D}_p \mathbf{F}_Q^H(:, L) \end{bmatrix} \quad (66)$$

According to the definition of the Fourier matrix, this matrix is further expressed as

$$\Psi = \begin{bmatrix} \sum_{m=1}^Q d_m & \dots & \sum_{m=1}^Q d_m e^{-j\frac{2\pi}{Q}(L-1)} \\ \sum_{m=1}^Q d_m e^{j\frac{2\pi}{Q}} & \dots & \sum_{m=1}^Q d_m e^{-j\frac{2\pi}{Q}(L-2)} \\ \vdots & \dots & \vdots \\ \sum_{m=1}^Q d_m e^{j\frac{2\pi}{Q}(L-1)} & \dots & \sum_{m=1}^Q d_m \\ \vdots & \dots & \vdots \\ \sum_{m=1}^Q d_m e^{-j\frac{2\pi}{Q}} & \dots & \sum_{m=1}^Q d_m e^{-j\frac{2\pi}{Q}L} \end{bmatrix} \quad (67)$$

which is a circulant matrix with the first column given by $\psi = \mathbf{F}_Q^H(\text{diag}(\mathbf{D}_p)) = \text{IFFT}\{\text{diag}(\mathbf{D}_p)\}$, and the first row given by $[\psi(0), \psi(1), \dots, \psi(Q - (L - 1))]$. This concludes the derivation of the matrix Ψ .

Appendix B. Derivation of $\mathbf{x}(\epsilon)$

Assuming that $\epsilon \cong \epsilon_0$ leads to

$$\begin{aligned} \mathbf{x}(\epsilon) &= \mathbf{T}_{sc} \mathbf{F}_K \Gamma^H(\epsilon) \Gamma^H(\epsilon_0) \mathbf{T}_K \mathbf{H} \mathbf{T}_{zp} \mathbf{F}_K^H \mathbf{s} + \eta \\ &\cong \mathbf{T}_{sc} \mathbf{F}_K \mathbf{T}_K \mathbf{H} \mathbf{T}_{zp} \mathbf{F}_K^H \mathbf{s} + \eta \\ &= \mathbf{T}_{sc} \mathbf{F}_K \mathbf{H}(1 : K, :) \mathbf{T}_{zp} \mathbf{F}_K^H \mathbf{s} + \eta \\ &= \mathbf{T}_{sc} \mathbf{F}_K \mathbf{H}(1 : K, :) \begin{bmatrix} \mathbf{F}_K^H \mathbf{s} \\ \mathbf{0}_L \end{bmatrix} + \eta \\ &= \mathbf{T}_{sc} \mathbf{F}_K \mathbf{H}(1 : K, 1 : K) \mathbf{F}_K^H \mathbf{s} + \eta \end{aligned} \quad (68)$$

where in the second transition we used the assumption that $\epsilon \cong \epsilon_0$, in the third transition we used the fact that $\mathbf{T}_K \mathbf{H} = \mathbf{H}(1 : K, :)$, in the fourth transition we used the definition of \mathbf{T}_{zp} to express the $P \times 1$ zero-padded transmitted signal, and in the fifth transition we multiplied the $K \times P$ matrix by the zero-padded $P \times 1$ transmitted signal. The $K \times K$ matrix $\mathbf{H}(1 : K, 1 : K)$ is expressed as

$$\mathbf{H}(1 : K, 1 : K) = \begin{bmatrix} h(0) & 0 & \dots & 0 \\ h(1) & h(0) & \dots & 0 \\ \vdots & \vdots & \dots & \vdots \\ h(L-1) & h(L-2) & \dots & 0 \\ 0 & h(L-1) & \dots & 0 \\ \vdots & 0 & \dots & \vdots \\ 0 & 0 & \dots & h(0) \end{bmatrix} \quad (69)$$

which is a Toeplitz matrix with the first column given by the $K \times 1$ vector $[h(0), h(1), \dots, h(L-1), \mathbf{0}_{K-L}^T]^T$. As any Toeplitz matrix is diagonalized by the discrete Fourier transform, then

$$\begin{aligned} \mathbf{F}_K \mathbf{H}(1 : K, 1 : K) \mathbf{F}_K^H &= \text{diag} \left(\mathbf{F}_K \begin{bmatrix} \mathbf{h} \\ \mathbf{0}_{K-L} \end{bmatrix} \right) \\ &= \text{diag} \left(\begin{bmatrix} \mathbf{F}_K(:, 1 : L) \\ \mathbf{F}_K(:, L+1 : K) \end{bmatrix}^H \begin{bmatrix} \mathbf{h} \\ \mathbf{0}_{K-L} \end{bmatrix} \right) \\ &= \text{diag}(\mathbf{F}_K(:, 1 : L) \mathbf{h}). \end{aligned} \quad (70)$$

Therefore we can now express $\mathbf{x}(\epsilon)$ as

$$\begin{aligned} \mathbf{x}(\epsilon) &= \mathbf{T}_{sc} \text{diag}(\mathbf{F}_K(:, 1 : L) \mathbf{h}) \mathbf{s} + \eta \\ &= \mathbf{T}_{sc} \text{diag}(\mathbf{s}) \mathbf{F}_K(:, 1 : L) \mathbf{h} + \eta. \end{aligned}$$

Observe that since

$$\mathbf{T}_{sc} \text{diag}(\mathbf{s}) \mathbf{F}_K(:, 1 : L) = \mathbf{D}_p \mathbf{F}_K(1 : G : K, 1 : L), \quad (71)$$

we obtain

$$\begin{aligned} \mathbf{x}(\epsilon) &= \mathbf{D}_p \mathbf{F}_K(1 : G : K, 1 : L) \mathbf{h} + \eta \\ &= \sqrt{Q} \mathbf{D}_p \mathbf{F}_Q(:, 1 : L) \mathbf{h} + \eta \end{aligned} \quad (72)$$

which is the result expressed in (14).

CRediT authorship contribution statement

Gilad Avrashi: Writing – original draft. **Alon Amar:** Writing – original draft. **Israel Cohen:** Writing – original draft.

References

- [1] Q. Zhan, H. Minn, New integer normalized carrier frequency offset estimators, *IEEE Trans. Signal Process.* 63 (14) (2015) 3697–3710.
- [2] F. Classen, H. Meyer, Frequency synchronization algorithms for OFDM systems suitable for communication over frequency selective fading channels, in: *The 44th IEEE Veh. Tech. Conf.*, Stockholm, Sweden, 1994.
- [3] B. Muquet, Z. Wang, G.B. Giannakis, M. De Courville, P. Duhamel, Cyclic prefixing or zero padding for wireless multicarrier transmissions? *IEEE Trans. Commun.* 50 (12) (2002) 2136–2148.
- [4] P.H. Moose, A technique for orthogonal frequency division multiplexing frequency offset correction, *IEEE Trans. Commun.* 42 (10) (1994) 2908–2914.
- [5] M. Morelli, U. Mengali, An improved frequency offset estimator for OFDM applications, *IEEE Commun. Lett.* (1999) 75–77.
- [6] T.M. Schmidl, D.C. Cox, Robust frequency and timing synchronization for OFDM, *IEEE Trans. Commun.* 45 (12) (1997) 1613–1621.
- [7] M. Morelli, U. Mengali, Carrier frequency estimation for transmissions over selective channels, *IEEE Trans. Commun.* 48 (9) (2000) 1580–1589.
- [8] J.J. van de Beek, M. Sandell, P.O. Borjesson, ML estimation of time frequency in OFDM systems, *IEEE Trans. Signal Process.* 45 (7) (1997) 1800–1805.
- [9] N. Lashkarian, S. Kiaei, Class of cyclic based estimators for frequency offset estimation of OFDM systems, *IEEE Trans. Commun.* (2000) 2139–2149.
- [10] S. Attallah, Blind estimation of residual carrier offset in OFDM systems, *IEEE Signal Process. Lett.* 11 (2) (2004) 216–219.
- [11] H. Liu, U. Tureli, A high efficiency estimator for OFDM communications, *IEEE Commun. Lett.* 2 (4) (1998) 104–106.
- [12] X. Ma, C. Tepedelenlioglu, G.B. Giannakis, S. Barbarossa, Non-data-aided carrier offset estimations for OFDM with null subcarriers: identifiability, algorithms, and performance, *IEEE J. Sel. Areas Commun.* 19 (12) (2001) 2504–2515.
- [13] U. Tureli, H. Liu, M.D. Zoltowski, OFDM blind carrier offset estimation: ESPRIT, *IEEE Commun. Lett.* 48 (2000) 1836–1847.
- [14] M. Luise, M. Marselli, R. Reggiani, Low complexity blind carrier frequency recovery for OFDM signals over frequency selective radio channels, *IEEE Trans. Commun.* 50 (7) (2002) 1182–1188.
- [15] Y. Yao, G.B. Giannakis, Blind carrier frequency offset estimation in SISO, MIMO, and multiuser OFDM systems, *IEEE Trans. Commun.* 53 (1) (2005) 173–183.
- [16] M. Stojanovic, J. Preisig, Underwater acoustic communication channels: propagation models and statistical characterization, *IEEE Commun. Mag.* 47 (1) (2009) 84–89.
- [17] B. Li, S. Zhou, M. Stojanovic, L. Freitag, P. Willett, Multicarrier communication over underwater acoustic channels with nonuniform Doppler shifts, *IEEE J. Ocean. Eng.* 33 (2) (2008) 198–209.
- [18] A.E. Abdelkareem, B.S. Sharif, C.C. Tsimenidis, Adaptive time varying Doppler shift compensation algorithm for OFDM-based underwater acoustic communication systems, *Elsevier Ad Hoc Netw.* 45 (2016) 104–119.
- [19] Z. Wang, G.B. Giannakis, Wireless multicarrier communications: where Fourier meets Shannon, *IEEE Signal Process. Mag.* 17 (3) (2000) 29–48.
- [20] Y.M. Aval, M. Stojanovic, Differentially coherent multichannel detection of acoustic OFDM signals, *IEEE J. Ocean. Eng.* 40 (2) (2015) 251–268.
- [21] J. Han, L. Zhang, Q. Zhang, G. Leus, Eigendecomposition-based partial FFT demodulation for differential OFDM in underwater acoustic communications, *IEEE Trans. Veh. Tech.* 67 (7) (2018) 6706–6710.
- [22] P.C. Carrascosa, M. Stojanovic, Adaptive channel estimation and data detection for underwater acoustic MIMO-OFDM systems, *IEEE J. Ocean. Eng.* 35 (3) (2010) 635–646.
- [23] A. Amar, G. Avrashi, M. Stojanovic, Low complexity residual Doppler shift estimation for underwater acoustic multicarrier communication, *IEEE Trans. Signal Process.* 65 (8) (2017) 2063–2076.
- [24] G. Avrashi, A. Amar, M. Stojanovic, I. Cohen, Eigenvalue decomposition based estimators of carrier frequency offset in multicarrier underwater acoustic communication, in: *IEEE ICASSP Conf.*, New Orleans, LA., 2017.
- [25] W. Zhou, Z.H. Wang, J. Huang, S. Zhou, Blind CFO estimation for zero-padded OFDM over underwater acoustic channels, in: *MTS/IEEE OCEANS Conf.*, Kona, Hawaii, 2011.
- [26] P.H. Moose, A technique for orthogonal frequency division multiplexing frequency offset correction, *IEEE Trans. Commun.* 42 (10) (1994) 2908–2914.
- [27] S. Yerramalli, M. Stojanovic, U. Mitra, Partial FFT demodulation: a detection method for highly Doppler distorted OFDM systems, *IEEE Trans. Signal Process.* 60 (11) (2012) 5906–5918.
- [28] X. Lurton, *An Introduction to Underwater Acoustics: Principles and Applications*, Springer Science & Business Media, 2002.
- [29] R.W. Gerchberg, W.O. Saxton, A practical algorithm for the determination of phase from image and diffraction plane pictures, *Optik* 35 (1972) 237–246.
- [30] J.R. Fienup, Reconstruction of an object from the modulus of its Fourier transform, *Opt. Lett.* 3 (1) (1978) 27–29.
- [31] P. Walk, H. Becker, P. Jung, OFDM channel estimation via phase retrieval, in: *IEEE 2015 49th Asilomar Conf. on Signals, Systems and Computers*, Pacific Grove, CA, USA., 2015.
- [32] Y. Shechtman, Y.C. Eldar, O. Cohen, H.N. Chapman, J. Miao, M. Segev, Phase retrieval with application to optical imaging: a contemporary overview, *IEEE Signal Process. Mag.* 32 (3) (2015) 87–109.
- [33] H.H. Bauschke, P. Combettes, D.R. Luke, Phase retrieval, error reduction algorithm, and Fienup variants: a view from convex optimization, *J. Opt. Soc. Am. A* 19 (7) (2002) 1334–1345.